第 34 卷第 11 期
2018 年 11 月

无 机 化 学 学 报
CHINESE JOURNAL OF INORGANIC CHEMISTRY

Vol.34 No.11
2057-2062

吡嗪缩氨基硫脲 Ni(Ⅱ)/Co(Ⅲ)配合物的合成、结构和 DNA 结合性质

吴 浩 王 元* 宋雨飞 张 玲 吴伟娜*

(河南理工大学化学化工学院,河南省煤炭绿色转化重点实验室,焦作 454000)

摘要: 合成并通过单晶衍射、元素分析及红外光谱表征了配合物[Ni(L)(OAc)] (**1**)和[Co(L)$_2$]Cl·4CH$_3$OH (**2**)的结构(HL 为 2-乙酰-3-甲基吡嗪-*N*-(4-氟苯基)缩氨基硫脲)。单晶衍射结果表明,配合物 **1** 中,Ni(Ⅱ)离子中心与缩氨基硫脲配体中的 NNS 供体和 1 个单齿醋酸根配位,形成扭曲的平面四边形配位构型;在配合物 **2** 中,Co(Ⅲ)离子中心与 **2** 个三齿缩氨基硫脲配体配位,拥有扭曲的八面体配位构型。此外,荧光光谱表明配合物 **1** 和 **2** 与 DNA 的相互作用强于配体。

关键词: Co(Ⅲ)配合物; DNA 结合; Ni(Ⅱ)配合物; 吡嗪; 缩氨基硫脲

中图分类号: O614.81$^+$2; O614.81$^+$3 **文献标识码**: A **文章编号**: 1001-4861(2018)11-2057-06

DOI:10.11862/CJIC.2018.253

Syntheses, Crystal Structures and DNA-Binding Properties of Ni(Ⅱ)/Co(Ⅲ) Complexes with Pyrazine Thiosemicarbazone Ligand

WU Hao WANG Yuan* SONG Yu-Fei ZHANG Ling WU Wei-Na*

(*College of Chemistry and Chemical Engineering, Henan Key Laboratory of Coal Green Conversion, Henan Polytechnic University, Jiaozuo, Henan* 454000, *China*)

Abstract: Two complexes [Ni(L)(OAc)] (**1**) and [Co(L)$_2$]Cl·4CH$_3$OH (**2**) (HL=2-aceto-3-methylpyrazine *N*-(4-fluorophenyl)thiosemicarbazone) have been synthesized and structurally determined by single-crystal X-ray diffraction, elemental analysis and IR spectroscopy. X-ray diffraction analysis results show that the Ni(Ⅱ) ion in complex **1** with a distorted square planar geometry is surrounded by one anionic TSC ligand with NNS donor set and one monodentate acetate. By contrast, Co(Ⅲ) ion coordinates with two tridentate TSC ligands, and thus possessing a distorted octahedron coordination geometry. Moreover, the fluorescence spectra indicate that the interactions of complexes **1** and **2** with DNA are stronger than that of the ligand HL. CCDC: 1848437, **1**; 1848438, **2**.

Keywords: Co(Ⅲ) complex; DNA-binding; Ni(Ⅱ) complex; pyrazine; thiosemicarbazone

Thiosemicarbazones (TSCs) and their metal complexes, especially the transition metal ones, have attracted intensity attention in the coordination chemistry because of their high biological and pharmaceutical activities, such as antibacterial, antiviral, antifungal, and antitumor activity[1]. On the other hand, pyrazine has been frequently used as key structural motif for the synthesis of various pharmaceutical agents[2]. As a result, including our group′s work, thiosemicarbazones (TSCs) involving pyrazine and their complexes have been found to display considerable antitumor activity[3-10].

Nevertheless, it is noted that the biological activities of TSCs often show a high dependence on

收稿日期:2018-06-13。收修改稿日期:2018-08-24。

国家自然科学基金(No.21001040)、河南省自然科学基金(No.182300410183,162300410011)、河南省教育厅高等校重点科研基金(No.19A150001)和河南理工大学校内基金(No.T2018-3,J2015-4)资助项目。

*通信联系人。E-mail:wangyuan08@hpu.edu.cn,wuwn08@hpu.edu.cn;会员登记号:S06N6704M1112(吴伟娜)。

their substituent. In this regard, it seems necessary to facilitate the activity of TSCs metals by changing the substitutes of TSCs themselves[4,11-12]. Herein a novel TSC (HL), namely 2-aceto-3-methylpyrazine *N*-(4-fluorophenyl)thiosemicarbazone, has been selected as the ligand. The structures and DNA-binding properties of its Ni(Ⅱ)/Co(Ⅲ) complexes have been discussed in detail.

1 Experimental

1.1 Materials and measurements

Solvents and starting materials for synthesis were purchased commercially and used as received. Elemental analysis was carried out on an Elemental Vario EL analyzer. The IR spectra (ν=4 000~400 cm^{-1}) were determined by the KBr pressed disc method on a Bruker V70 FT-IR spectrophotometer. ^1H NMR spectra of HL was acquired with Bruker AV400 NMR instrument in DMSO-d_6 solution with TMS as internal standard. The UV spectra were recorded on a Purkinje General TU-1800 spectrophotometer. The interactions between three compounds and ct-DNA are measured using literature method[13] via emission spectra on a Varian CARY Eclipse spectrophotometer.

1.2 Preparations of the ligand and complexes 1 and 2

As shown in Scheme 1, the ligand HL was prepared by condensation of 2-aceto-3-methylpyrazine (1.36 g, 0.01 mol) and 4-fluorophenyl thiosemicarbazide (1.85 g, 0.01 mol) in ethanol solution (30 mL) with continuous stirring at room temperature for 3 h. Yield: 2.08 g (82%). Elemental analysis Calcd. for $C_{14}H_{14}N_5SF$(%): C, 55.44; H, 4.62; N, 23.10. Found (%): C, 55.62; H, 4.56; N, 22.99. FT-IR (cm^{-1}): ν(C=S) 843, $\nu(C=N)_{imine}$ 1 606, $\nu(C=N)_{pyrazine}$ 1 546. ^1H NMR (400 MHz, DMSO-d_6): δ 10.91 (s, 1H, NH), 10.01 (s, 1H, NH), 8.52~8.54 (m, 2H, pyrazine-H), 7.57~7.61 (m, 2H)/7.17~7.21 (m, 2H) for phenyl-H, 2.77 (3H, s, CH_3), 2.44 (3H, s, CH_3).

Complexes **1** and **2** were generated by reaction of HL (5 mmol) with equimolar of $Ni(OAc)_2$ and $CoCl_2$ in CH_3OH (10 mL) solution, respectively. Crystals of **1** and **2** suitable for X-ray diffraction analysis were obtained by evaporating the corresponding reaction solutions at room temperature.

1: brown blocks. Anal. Calcd. for $C_{16}H_{16}O_2N_5SFNi$ (%): C, 45.70; H, 3.80; N, 16.66. Found(%): C, 45.56; H, 3.88; N, 16.73. FT-IR (cm^{-1}): ν(C=S) 831, ν(C=N) 1 608, $\nu(C=N)_{pyrazine}$ 1 543.

2: brown plates. Anal. Calcd. for $C_{32}H_{42}O_4N_{10}F_2S_2ClCo$(%): C, 46.42; H, 5.07; N, 16.92. Found(%): C, 46.50; H, 4.97; N, 17.01. FT-IR (cm^{-1}): ν(C=S) 836, ν(C=N) 1 618, $\nu(C=N)_{pyrazine}$ 1 541.

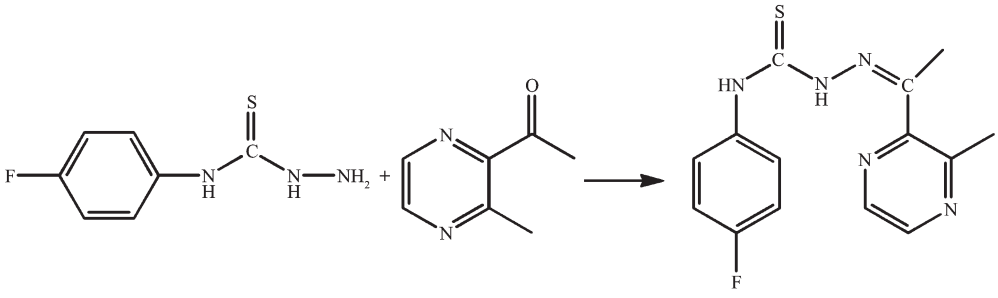

Scheme 1 Synthetic route for HL

1.3 X-ray crystallography

The X-ray diffraction measurement for complexes **1** (Size: 0.10 mm×0.08 mm×0.08 mm) and **2** (Size: 0.15 mm×0.14 mm×0.06 mm) was performed on a Bruker SMART APEX Ⅱ CCD diffractometer equipped with a graphite monochromatized Mo $K\alpha$ radiation (λ= 0.071 073 nm) by using φ-ω scan mode. Semi-empirical absorption correction was applied to the intensity data using the SADABS program[14]. The structures were solved by direct methods and refined by full matrix least-square on F^2 using the SHELXTL-97 program[15]. All non-hydrogen atoms were refined anisotropically. All H atoms were positioned geometrically and refined using a riding model. Details of the

Table 1　Crystal data and structure refinement for complexes 1 and 2

	1	2
Empirical formula	$C_{16}H_{16}FN_5NiO_2S$	$C_{32}H_{42}ClCoF_2N_{10}O_4S_2$
Formula weight	420.11	827.26
T / K	296(2)	293(2)
Crystal system	Monoclinic	Triclinic
Space group	$P2_1/c$	$P\bar{1}$
a / nm	1.152 32(13)	1.170 49(15)
b / nm	0.870 16(10)	1.207 64(14)
c / nm	1.766 5(2)	1.455 99(17)
α / (°)		108.472(2)
β / (°)	101.515(2)	95.138(2)
γ / (°)		96.239(2)
V / nm^3	1.735 6(3)	1.923 6(4)
Z	4	2
D_c / (g·cm^{-3})	1.608	1.428
Absorption coefficient / mm^{-1}	1.270	0.684
F(000)	864.0	860
Reflection collected, Unique (R_{int})	8 303, 3 058 (0.021 9)	9 851, 6 739 (0.015 7)
Data, restraint, parameter	3 058, 0, 238	6 739, 0, 481
Goodness-of-fit (GOF) on F^2	1.017	1.016
Final R indices [$I>2\sigma(I)$]	R_1=0.026 8, wR_2=0.068 0	R_1=0.035 4, wR_2=0.087 9
R indices (all data)	R_1=0.033 1, wR_2=0.071 8	R_1=0.047 6, wR_2=0.095 5

crystal parameters, data collection and refinements for complexes **1** and **2** are summarized in Table 1.

CCDC: 1848437, **1**; 1848438, **2**.

2　Results and discussion

2.1　Crystal structures description

A diamond drawing for complexes **1** and **2** is shown in Fig.1. Selected bond distances and angles are listed in Table 2. The lengths of C-S bond are in the range of 0.175 4(2)~0.175 0(2) nm in complexes **1** and **2**, showing that the ligand HL has thiolated and deprotonated in both complexes[16].

As shown in Fig.1a, the central Ni(Ⅱ) ion in complex **1** is surrounded by one anionic TSC ligand with NNS donor set and one monodentate acetate, giving a slightly distorted planar geometry (RMS deviation: 0.001 85 nm). The distances of coordination bonds were in the normal range (0.183 80(16)~0.215 57(6) nm). In the crystal, the intermolecular N–H⋯O hydrogen bonds (N5–H5⋯O2^{i}, with D⋯A distance being 0.291 8(2) nm, D–H⋯A angle being 152.0°; Symmetry codes: ^{i} 2–x, 0.5+y, 2.5–z) link the molecules into zig-zag chains along b axis, as illustrated in Fig.1b.

The asymmetric unit of complex **2** contains one discrete cationic Co(Ⅲ) complex (Fig.1c), in which the center Co(Ⅲ) ion is coordinated by two tridentate TSC ligands, and thus possessing a distorted octahedron coordination geometry. Although complex **2** is prepared using $CoCl_2$, there exists one free chloride anion in the outside of the complex for charge balance. This is a normal phenomenon in the Co(Ⅲ)complexes with TSC ligands in the literature[17]. In the solid state, crystal methanol molecules and free chloride anions link the complex cations into a centrosymmetric supramolecular dimer (Fig.1d) through intermolecular O–H⋯O (O4–H4⋯O3, with D⋯A distance being 0.281 9(3) nm, D–H⋯A angle being 160.2°), N–H⋯O (N5–H5⋯O2, with D⋯A distance being 0.283 2(3) nm, D–H⋯A angle being 173.0°; N10–H10⋯O4, with D⋯A distance being 0.291 8(3) nm, D–H⋯A angle being 175.0°) and O–H⋯Cl hydrogen bonds (O1–H1⋯Cl1,

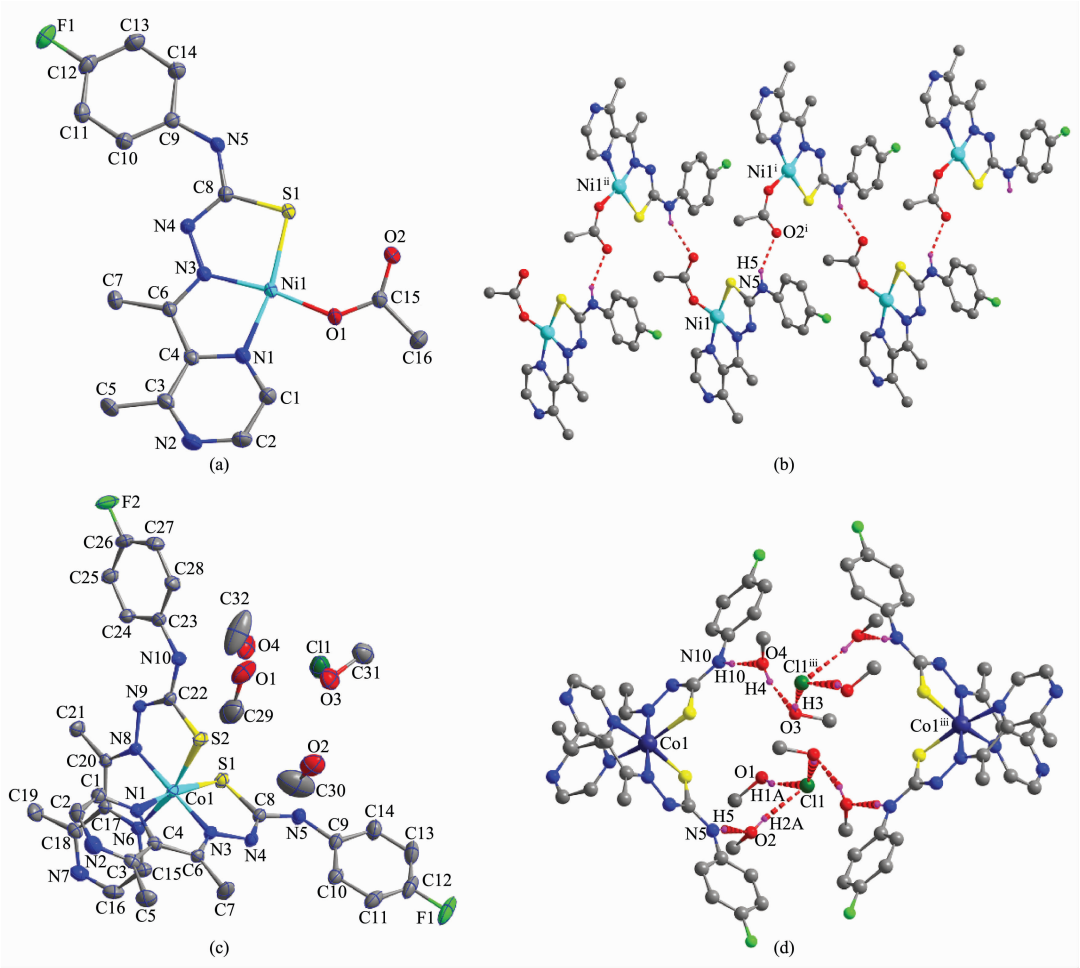

Hydrogen bonds shown in dashed line; H atoms for C-H bonds are omitted for clarity; Symmetry codes: [i] 2−*x*, 0.5+*y*, 2.5−*z*; [ii] 2−*x*, −0.5+*y*, 2.5−*z*; [iii] 1−*x*, 1−*y*, −*z*

Fig.1 ORTEP drawing of **1** (a) and **2** (c) with 30% thermal ellipsoids; (b) Zig-zag chain-like structure along *b* axis formed via N–H···O hydrogen bonds in complex **1**; (d) Centrosymmetric supramolecular dimer in complex **2**

Table 2 Selected bond lengths (nm) and angles (°) in complexes 1 and 2

		1			
Ni1-N1	0.191 67(17)	Ni1-N3	0.183 80(16)	Ni1-S1	0.215 57(6)
Ni1-O1	0.184 43(16)				
N1-Ni1-N3	82.49(7)	O1-Ni1-S1	100.42(5)	N3-Ni1-S1	87.74(5)
N1-Ni1-S1	169.41(6)	O1-Ni1-N3	170.78(8)	O1-Ni1-N1	89.65(7)
		2			
Co1-N3	0.187 97(17)	Co1-N8	0.188 51(17)	Co1-N1	0.194 85(19)
Co1-N6	0.196 19(19)	Co1-S1	0.222 10(7)	Co1-S2	0.222 37(7)
N3-Co1-N8	178.93(8)	N3-Co1-N1	81.80(8)	N8-Co1-N1	99.27(8)
N3-Co1-N6	98.29(8)	N8-Co1-N6	81.74(8)	N1-Co1-N6	88.45(8)
N3-Co1-S1	86.47(6)	N8-Co1-S1	92.46(6)	N1-Co1-S1	168.16(6)
N6-Co1-S1	91.73(6)	N3-Co1-S2	93.68(6)	N8-Co1-S2	86.33(6)
N1-Co1-S2	90.87(6)	N6-Co1-S2	167.79(6)	S1-Co1-S2	91.42(3)

with D···A distance being 0.320 0(3) nm, D–H···A angle being 164.7°; O2–H2···Cl1, with D···A distance being 0.312 0(3) nm, D–H···A angle being 172.6°; O1–H1···Cl1^{iii}, with D···A distance being 0.313 2(3) nm, D–H···A angle being 171.9°; Symmetry codes: ^{iii} 1–x, 1–y, –z).

2.2 IR spectra

The most useful infrared spectral bands for determining the mode of coordination of the ligands are the ν(C=N)$_{imine}$, ν(C=N, pyrazine) and ν(C=S). Such three bands of the free TSC ligand is found at 1 606, 1 546 and 843 nm^{-1}, while they shift to lower frequency in complexes **1** and **2**, clearly indicating the coordination of imine nitrogen, pyrazine nitrogen and sulfur atoms[13,18]. It is in accordance with the X-ray diffraction analysis result.

2.3 UV spectra

The UV spectra of the ligand HL, complexes **1** and **2** in CH_3OH solution (Concentration: 10 μmol·L^{-1}) were measured at room temperature (Fig.2). The spectrum of HL features only one main band located around 305 nm (ε=59 100 L·mol^{-1}·cm^{-1}), which could be contributed to the characteristic π-π* transition of pyrazine[13]. In complexes **1** and **2**, this band blue-shifted to 253 nm (ε=34 900 L·mol^{-1}·cm^{-1}) and 255 nm (ε=89 600 L·mol^{-1}·cm^{-1}). Moreover, complexes **1** and **2** exhibit new peaks located at 395 nm (ε=22 800 L·mol^{-1}·cm^{-1}) and 407 nm (ε=41 600 L·mol^{-1}·cm^{-1}), respectively, corresponding to the ligand-to-metal charge transfer (LMCT)[19]. All facts support the coordination of ligand HL in both complexes.

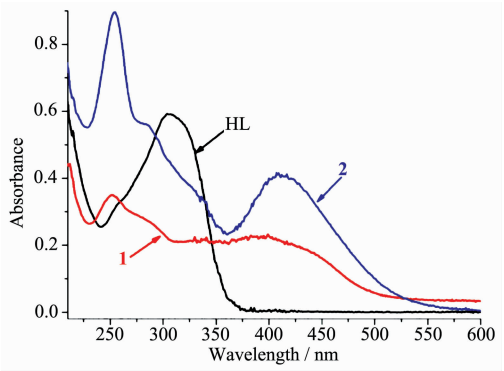

Fig.2　UV spectra of the ligand HL, complexes **1** and **2** in CH_3OH solution at room temperature

2.4 EB-DNA binding study by fluorescence spectrum

It is well known that EB can intercalate nonspecifically into DNA, which causes it to fluoresce strongly. Competitive binding of other drugs to DNA and EB will result in displacement of bound EB and a decrease in the fluorescence intensity[18-19]. The effects of the ligand and complexes on the fluorescence spectra of EB-DNA system are presented in Fig.3, the fluorescence intensities of EB bound to ct-DNA at about 600 nm show remarkable decreasing trends with the increasing concentration of the tested compounds, indicating that some EB molecules are released into solution after the exchange with the compounds. The quenching of EB bound to DNA by the compounds is in agreement with the linear Stern-Volmer equation: I_0/I=1+$K_{sq}r$[20], where I_0 and I represent the fluorescence intensities in the absence and presence of quencher, respectively; K_{sq} is the linear Stern-Volmer quenching constant; r is the ratio of the concentration of quencher

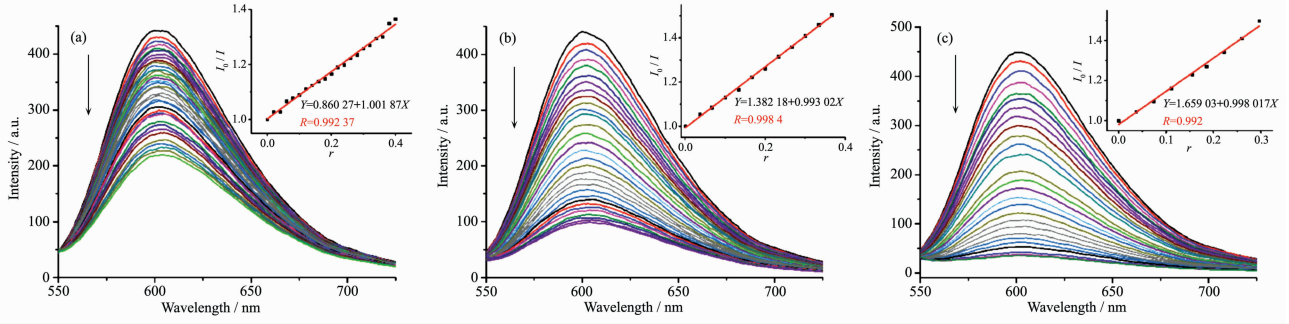

Arrow shows the fluorescence intensities change of EB-DNA system upon increasing tested compound concentration; Inset: plot of I_0/I versus r, r=$c_{quencher}/c_{DNA}$

Fig.3　Emission spectra of EB-DNA system in the absence and presence of ligand HL (a), complexes **1** (b) and **2** (c)

and DNA. In the quenching plots of I_0/I versus r, K_{sq} values are given by the slopes. The K_{sq} values are 0.860, 1.382 and 1.659 for the ligand HL, complexes **1** and **2**, respectively. The results indicate that interactions of the complexes with DNA are stronger than that of the ligand HL, probably due to the higher rigidity and metal-ligand synergism effect of the complexes.

References:

[1] Rezaeivala M, Keypour H. *Coord. Chem. Rev*., **2014**,**280**:203-253

[2] Casanova I, Duran M L,Viqueira J, et al. *Dalton Trans*., **2018**, **47**:4325-4340

[3] Qi J, Deng J, Qian K, et al. *Eur. J. Med. Chem*., **2017**,**134**: 34-42

[4] Qi J, Su L, Gou Y, et al. *Eur. J. Med. Chem*., **2015**,**96**:360-368

[5] Zeglis B M, Divilov V, Lewis J S. *J. Med. Chem*., **2011**,**54**: 2391-2398

[6] Li M X, Zhang L Z, Yang M, et al. *Bioorg. Med. Chem. Lett*., **2012**,**22**:2418-2423

[7] Li M X, Zhang L Z, Zhang D, et al. *Eur. J. Med. Chem*., **2011**,**46**:4383-4390

[8] Li M X, Chen C L, Zhang D, et al. *Eur. J. Med. Chem*., **2010**, **45**:3169-3177

[9] Rogolino D, Cavazzoni A, Gatti A, et al. *Eur. J. Med. Chem*., **2017**,**128**:140-153

[10]Lovejoy D B, Sharp D M, Seebacher N, et al. *J. Med. Chem*., **2012**,**55**:7230-7244

[11]Matesanz A I, Leitao I, Souza P. *J. Inorg. Biochem*., **2013**,**125**: 26-31

[12]Matesanz A I, Souza P. *Inorg. Chem. Commun*., **2013**,**27**:5-8

[13]MAO Pan-Dong(毛盼东), ZHAO Xiao-Lei(赵晓雷), SHAO Zhi-Peng(邵志鹏), et al. *Chinese J. Inorg. Chem.*(无机化学学报), **2017**,**33**:890-896

[14]Sheldrick G M. *SADABS*, University of Göttingen, Germany, **1996**.

[15]Sheldrick G M. *SHELX*-97, *Program for the Solution and the Refinement of Crystal Structures*, University of Göttingen, Germany, **1997**.

[16]Ramachandran E, Thomas S P, Poornima P, et al. *Eur. J. Med. Chem*., **2012**,**50**:405-415

[17]MAO Pan-Dong(毛盼东), YAN Ling-Ling(闫玲玲), WANG Wen-Jing(王文静), et al. *Chinese J. Inorg. Chem.*(无机化学学报), **2016**,**32**:555-560

[18]Nakamoto K. *Infrared and Raman Spectra of Inorganic and Coordination Compounds*. 4*th Ed*. New York: Wiley, **1986**: 257

[19]MAO Pan-Dong(毛盼东), HAN Xue-Feng(韩学锋), WU Wei-Na(吴伟娜), et al. *Chinese J. Inorg. Chem.*(无机化学学报), **2016**,**32**:161-166

[20]Yang Z Y, Wang Y, Wang Y. *Bioorg. Med. Chem. Lett*., **2007**,**17**:2096-2101